

Development of A Low-Cost Arduino-Based 12-Lead Ecg Acquisition System And Accompanied Labview Application



Son Nguyen Van, Duc Trinh Quang, Giang Nguyen Hoai

Abstract: In this paper, the design of a real-time digital multi-channel ECG signal acquisition system is presented. With the purpose of fabrication towards a simple, compact and low-cost tool for bioelectrical signal processing laboratories, the system is developed to acquire the 12 leads ECG signals and converted to numerical data based on an Arduino module named as Leonardo equipped 12 channels ADC. To observe the ECG waves, the ECG signals are amplified through designed amplifiers with the gain of 60 dB. To reduce the effects from the DC component as well as the baseline wandering and the high frequency noise, the active analog bandpass filter ranged in 0,05 Hz to 100 Hz was designed. The power line noise of 50 Hz also decreased with an active analog bandstop filter with attenuation -38 dB. Under the PC application was built using Labview programming, the low-cost digital ECG signal acquisition system was demonstrated with the requirement of observation in real-time. To clarify the small wave in the digital ECG signal, the limitation of the analog signal processing is improved through the digital filters parameterized in the software to increase the SNR from 1.4 dB to 27.6 dB. Practically, the system is evaluated through a series of experiments on a volunteer person resulting the ECG data is recorded and stored in a TDMS file. Since the system is designed as opened-system, a series of developments towards various applications in biomedical diagnosis based on digital signal analysis techniques is promised to be feasible in the near future.

Keywords: Arduino application, Low-cost ECG 12 leads, Labview

I. INTRODUCTION

The ECG instruments were designed, fabricated by many manufacturers as commercial products and used as popular devices in hospital for diagnostic cardiovascular diseases [1]. However, these devices often are closed-system and difficult to employ specific analysis purpose since their data is recorded through software with authorized protection and printed out to chart medical thermal paper. The numerical

data is necessary to expose for novel application or development of new analytic techniques.

In practice, there are a lot of single channel ECG circuits were implemented in laboratories [5, 6]. Nevertheless, most of them use only three electrodes to measure one of three bipolar limb leads. The signal includes some basic contents but does not respond whole cardiovascular activities of human bodies, hence, it is not enough the information for full diagnostics [2].

For the reason of study on ECG analytic technique development in the future, a low-cost and opened digital ECG measurement system possibly equipped 12 leads should be designed and practical developed. The system requires obtained data from twelve ECG leads in real time and stores it into the popular format files. Because the aims, this report presents the design of the digital low-cost ECG system allowing the data collection for further researches. These data then can be saved to a computer popular format file to be the object for the other researches.

II. METHODS

2.1 Theoretical Approaches

Typically, a standard ECG measurement instrument has twelve leads. Each of the twelve ECG leads records the electrical signal from a heart responding to a different aspect, which contains the different anatomical activity of the heart. A total of twelve leads fully provide the information to cardiologists during examination or treatment. These twelve leads comprises three bipolar limb leads, three augmented unipolar limb leads and six precordial leads [3].

The three bipolar limb leads: consist of leads I, II and III. Each of the leads is the electric potential difference between two out of three electrodes: left arm (LA), right arm (RA) and left leg (LL) [4].

$$I = LA - RA \quad (1)$$

$$II = LL - RA \quad (2)$$

$$III = LL - LA \quad (3)$$

The three augmented unipolar limb leads: include lead aVR, aVL, aVF, computed from the same 3 electrodes as three limb leads, they use Goldberger's central terminal as their negative pole which is a combination of inputs from other two limb electrodes [5].

$$aVR = RA - \frac{LA+LL}{2} \quad (4)$$

$$aVL = LA - \frac{RA+LL}{2} \quad (5)$$

$$aVF = LL - \frac{RA+LA}{2} \quad (6)$$

Revised Manuscript Received on October 30, 2019.

* Correspondence Author

Son Nguyen Van, Hanoi Open University, Hanoi, Vietnam.
sonnv@hou.edu.vn

Duc Trinh Quang*, Hanoi University of Science and Technology, Hanoi, Vietnam. duc.trinhquang@hust.edu.vn

Giang Nguyen Hoai, Hanoi Open University, Hanoi, Vietnam.
giangnh@hou.edu.vn

© The Authors. Published by Blue Eyes Intelligence Engineering and Sciences Publication (BEIESP). This is an open access article under the CC BY-NC-ND license (<http://creativecommons.org/licenses/by-nc-nd/4.0/>)

The six precordial leads:

The six chest electrodes act as the positive poles for the six correspondent precordial leads compared with Wilson’s central terminal. These leads include V1, V2, V3, V4, V5 and V6 [6]. Although ECG signal has twelve leads, it is not necessary to build the hardware includes twelve separate channels circuit. Several leads can be represented by calculation from the others.

From formulas (1) (2) and (3), we can easily find out the relationship among limb leads. Lead II is equal to the sum of leads I and III and is given:

$$II = I + III \quad (7)$$

Inserting equation (1), (2), and (3) into equation (4), (5), and (6), aVR, aVL, aVF can be expressed by:

$$aVR = \frac{-(I + III)}{2} \quad (8)$$

$$aVL = \frac{I - III}{2} \quad (9)$$

$$aVF = \frac{II + III}{2} \quad (10)$$

Consequently, for the twelve leads ECG system, we just need to design circuit with channels for eight leads and the others possibly computed in software. These direct eight leads are lead I, III and six precordial leads (V1, V2, V3, V4, V5 and V6). The four leads reconstructed by software are: lead II, aVR, aVL and aVF.

2.2 The system

Since the ECG signal is very weak, approximately from 1 mV to 5 mV and the frequency is ranged from 0.05 Hz – 100 Hz [7]. For diagnostic applications of cardiovascular disease, the signal has to be amplified. During the amplification, as an electrical signal, ECG is interfered from many kinds of noises. The main noise sources are electrical noise from body muscle (EMG-Electromyography), baseline wandering from impedance matching between skin and electrode, noise of 50 Hz from electricity power lines, and the electromagnetic microwave from telecommunication systems [7].

To reduce the noises, the active filters need to be integrated with the amplifiers. For the discretization, since the maximum frequency of ECG signals is 100 Hz, the sampling frequency must be more than 200 Hz. In our system, the sampling frequency is set it as 350 Hz, which can satisfy the Nyquist sampling theorem. With eight channels, to collect the numerical data from the signal with the sampling frequency, a microcontroller integrated with ADC (Analog to Digital Converter) module designed and named as Arduino Leonardo was used. Each analog input provides 10 bits of measurement resolution with the voltage input ranged in 0 to 5V. Some major parameters is summarized in table 1 and the block function of the proposed system is shown in figure 1 illustrating the block diagram of the whole system.

Table- I: The specifications of system [12]

Parameter	Description
G = 60 dB	Gain of whole system
Filters	Highpass, lowpass, bandstop
ADC resolution	10 bit
Channel number	8 channels
Sampling frequency	350Hz (each channel)
Electrodes type	10 adhesive electrodes

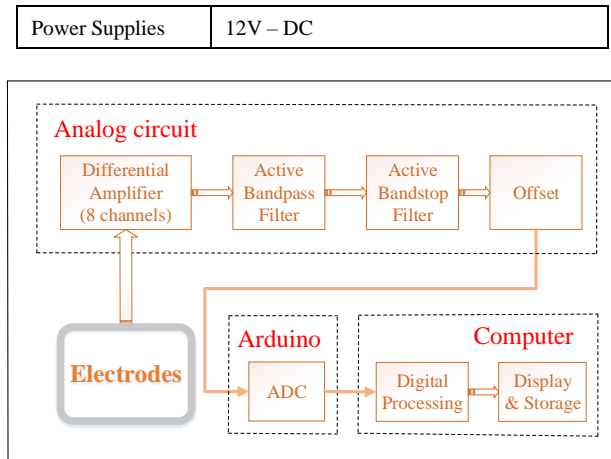


Fig. 1. The system Block diagram

For acquisition the ECG data, the system collected the measured signal through 8 channels established from 10 electrodes, including 4 electrodes placed on limbs and 6 electrodes placed on chest. The leads I and III are formed by two of three electrode in right hand, left hand and left leg. Whereas, the six precordial leads measure the signal from six positions in front of chest in comparison with a reference point. This point is obtained by connection of the limb leads to a common point through each 100 KΩ resistor so called Wilson central terminal [6]. The diagram of the connection is shown in figure 2.

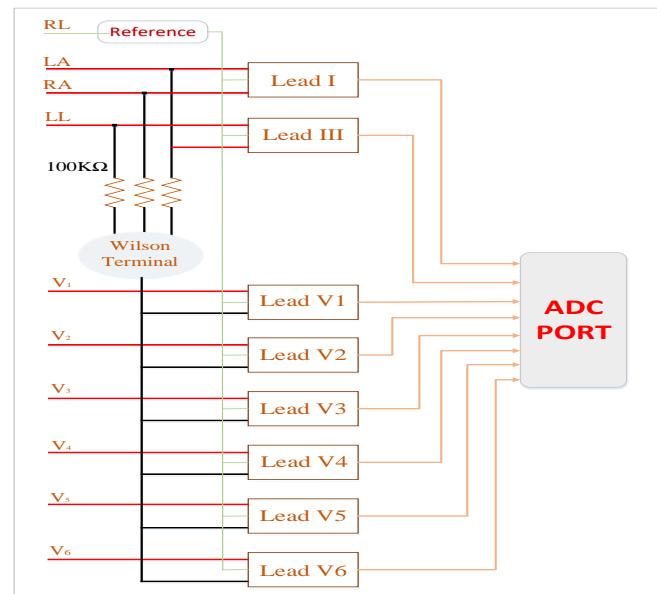


Fig. 2. 8 channel configuration diagram

2.3 The amplifiers and filters

Because of the weakness and the range of the ECG signal, as the typical ECG measurement system, this system also need 8 amplifiers adapted with the measurement range of 0 to 5 V. The typical ECG signal is ranged on 1 to 5 mV [7], hence, for the range of 0 to 5 V, the gain of each amplifier should be 60 dB. Since the gain and the configuration of the each amplifier are similar to the other, a design for a channel is presented as the unit module. The figure 3 shows the schematic of the analog amplifier circuit.



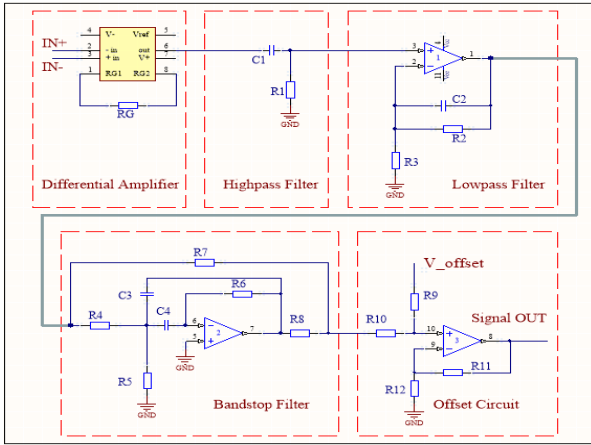


Fig. 3. The schematic of amplifiers and filters

i. Differential amplifier

To reduce the noise as well as increase the SNR (signal to noise ratio) during the amplification, the amplifier is arranged to be 3 stages. The first stage of these amplifier is the differential amplifier (INA128) with the gain set to be 40 dB through a resistor RG whose value of 400 Ω connected between pin 1 and pin 8.

ii. Highpass filter

A typical measured ECG signal usually contains AC (Alternating Current) and DC (Direct Current) components [8] which the AC is the component is validity for diagnosis. Therefore, in this scheme, a passive highpass filter is applied at the output of instrumentation amplifier (figure 3) to eliminate the DC components and minimize the baseline wandering occurred due to the respiration or the motion of the body. The high cut-off frequency of this filter is calculated in the formula as below [9]:

$$f_c = \frac{1}{2\pi R_1 C_1} \quad (11)$$

According to the formula (11), with R1 = 2 MΩ and C1 = 470 nF, the high cut-off frequency (fc) is estimated as about 0.16 Hz.

To evaluate the filter circuit, the Bode analyzer function was investigated with both the experimental measurement and the simulation data of the frequency response. The comparison has been shown in figure 4, Since the frequency range of the ECG signal is varied from 1 Hz to 100 Hz, and with the frequency step of 1 Hz of a function generator was used to measure the response, the frequency response curve in ranged in 1 Hz to 100 Hz is presented. As the figure shown, in the pass range, the difference between the mathematical simulation and the practical model is small to be neglected in the pass range.

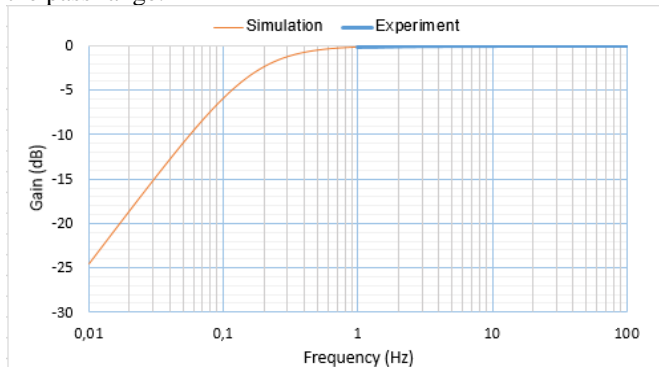


Fig. 4. The frequency response of highpass filter

In the stop range, because of the limitation of the hardware devices, the attenuation response could not be evaluated practically. Based on the definition of the transfer function filter, the attenuation can be determined as [9]:

$$H = \frac{V_{out}}{V_{in}} = R_1 / \sqrt{R_1^2 + ZC_1^2} \quad (12)$$

At the frequency of 1 Hz, ZC1 = 1 / (2πfC1) = 338 KΩ and R1 = 2 MΩ, so the H value is estimated to be 0.986, then the value can convert to decibels scale as:

$$H = 20 * \text{Log } 0.986 \approx 0.123 \text{ dB}$$

Beside it, the experimental curve shows that the attenuation at frequency 1 Hz is approximately 0dB, close to theoretical estimation. The effectiveness of the filter will be demonstrated and discussed in the result section of this report.

Active lowpass filter

To remove the unwanted wave from high frequencies, a lowpass filter integrated with an amplifier is considered. This active filter is designed as the second order to attenuate the noises in higher frequencies more stronger. On the other hands, an amplifier is also combined with constant gain. The low cut-off frequency can be written as [9]:

$$f_c = \frac{1}{2\pi R_2 C_2} \quad (13)$$

The cut-off frequency is given at 100 Hz with a resistor R2 = 1.6 MΩ and C2 = 1 nF. For a non-inverting amplifier circuit, the magnitude of the voltage gain for the filter is given as a function of ratio between the feedback resistor (R2) and the input resistor (R3) [9]:

$$G = 1 + \frac{R_2}{R_3} \quad (14)$$

With the values of R2 has shown above and the value of R3 is chosen as 400 KΩ, the gain of the amplifier is obtained as 5 or 14 dB (20*log5) approximately. Figure 5 shows the numerical simulation and the experimental frequency response ranged in 1 Hz to 1 KHz. At the cut-off frequency of 100 Hz, the gain is approximately 11 dB and drops to -27 dB at frequency of 1kHz

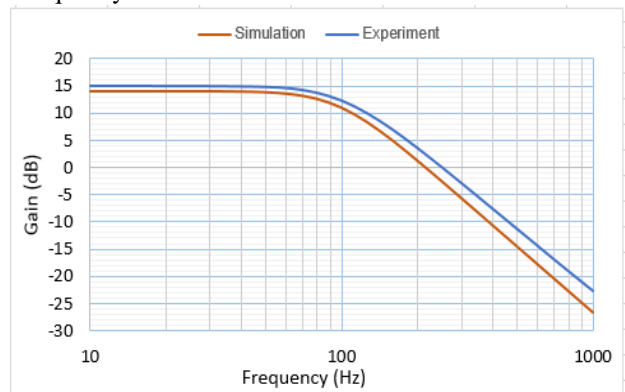


Fig. 5. The frequency response of active lowpass filter

As the figure shown, the gain of amplifier is designed as 15 dB and the cut-off frequency is located on 100 Hz. At frequency 1 KHz, the attenuation is approximately -23 dB (4 dB less than the theoretical simulated value).

Bandstop filter

The bandstop filter in this system aims to reduce the power line noise of 50 Hz. In this work, a second order active bandstop filter is considered. The central frequency is expressed as [9]:



$$f_c = \frac{1}{2\pi\sqrt{(R4/R5) \cdot R6 \cdot C3 \cdot C4}} \quad (15)$$

With the values of resistors are chosen as $R4 = R5 = 14.5 \text{ K}\Omega$, $R6 = 29 \text{ K}\Omega$ and the capacitor values of $C3 = C4 = 220 \text{ nF}$, the central frequency f_0 is determined at 50 Hz. At this frequency, the attenuation is -46 dB. The quality factor Q is $1(\pi \cdot f_0 \cdot R6 \cdot C3)$, the low cut-off and high cut-off frequency are given by [9]:

$$f_{c1} = f_0 \cdot \sqrt{1 + \left(\frac{1}{2Q}\right)^2} - \frac{f_0}{2Q} \quad (16)$$

$$f_{c2} = f_0 \cdot \sqrt{1 + \left(\frac{1}{2Q}\right)^2} + \frac{f_0}{2Q} \quad (17)$$

Hence, the $f_{c1} = 31 \text{ Hz}$ and $f_{c2} = 80 \text{ Hz}$. The magnitude of the voltage gain for the filter is determined by two resistors $R7$ and $R8$ [9]:

$$G = \frac{V_{out}}{V_{in}} = \frac{R8}{R7 + R8} \quad (18)$$

Setting the resistor values of $R7 = R8 = 10 \text{ K}\Omega$, the output voltage is half of the input voltage ($20\log 0.5 = -6 \text{ dB}$).

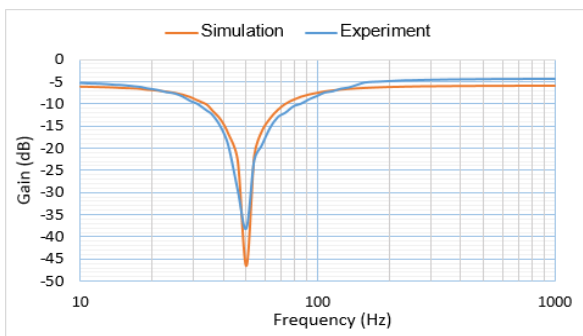


Fig. 6. The frequency response of bandstop filter

The comparison of the simulation data and the measurement data of the frequency response of the bandstop filter is shown in figure 6. The central frequency is located on 50Hz with attenuation -38 dB. Also, the low cut-off and high cut-off frequency of filter are estimated as 28 Hz and 82 Hz. The difference in the practical model and the theoretical model possibly come from the nonlinear response of the electronic device [10]. However, with the error of -5 dB approximately for the attenuation at the center frequency, the remained noise can be eliminated by the digital filters installed in Labview. Offset circuit

Since the output of circuit has negative components, an offset circuit is required to adjust the level of the signal to a specified offset voltage for adaptation with the measurement range set on the ADC. The offset circuit is designed simply based on the application of summing amplifier. The voltage of V_{offset} is tuned to adjust the level of most negative value of the signal to be zero.

The values and the ratios of the signal amplitude measured from the leads contain the clinical information validating to diagnosis. Therefore, the gain of the amplifier should be set as the same. To ensure all of 8 channels have the same amplifier gain, the frequency responses of 8 channels are measured in ranged of 1 Hz – 100 Hz. Figure 7 shows the gain values of 8 channels is approximately 14.6 dB with small errors to be negligible.

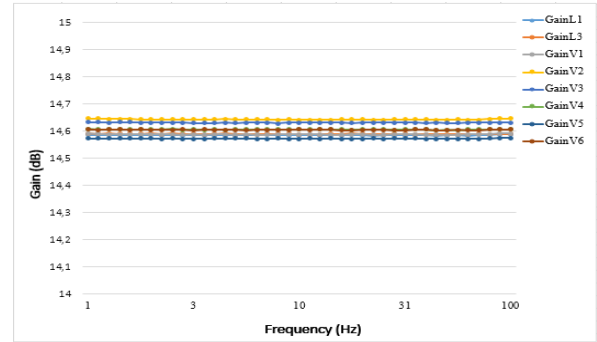


Fig. 7. The frequency responses of the amplifiers

2.4 The Labview program

The goal of this system is ECG measurement data acquisition for further development of analysis techniques. Therefore, a software is need to be programmed to do the processes. Beside it, since the analog filters attenuated the noise low, the digital filters possibly perform the fine processes to increase SNR of the signal. For this purpose, the program of the software is designed in Labview with the block diagram function shown in figure 8.

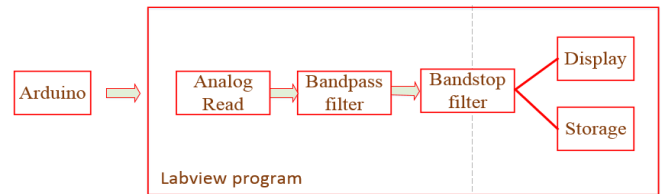


Fig. 8. Labview block function diagram

The program includes 4 main modules: the signal reader, signal processing (filters), display, and the storage. To read the digital signal, the Labview toolbox named as Linx made by Makerhub was used [11].

This tool support the control of Labview for Arduino modules to collect the digital signal discretized by ADC component in the module and transfer the data through a computer USB serial port [12]. The Arduino Leonardo module reserved with 12 channels ADC being available for the 8 analog channels of this system. To improve the SNR, the digital filters of bandpass and bandstop is designed with the parameters shown in table 2. The display and the storage procedure were programmed with the original functions equipped from NI Labview. The stored data file type is TDMS (Technical data management streaming) format, this data can be browsed by Microsoft Excel.

Table- II: The digital filter parameters

Filters	Function	Parameters
Bandpass Butterworth	Remove noises out of range from 0 – 100 Hz	Fc low = 0.05 Hz Fc high = 100 Hz Order = 6
Bandstop Butterworth	Remove 50 Hz noise	Fc low = 48 Hz Fc high = 52 Hz Order = 6

To evaluate the efficiency of the filters quantitatively, the frequency response was measured with the excitation of sinusoidal wave ranged from 1 Hz to 500 Hz then compare with the simulation data. The sine waves were generated by NI ELVIS II fed into Arduino analog pin directly, converted to digital wave.



Then, the amplitude of the signal were used to calculate the attenuation values interpolated to be shown in figures 10 and 11. The diagram of the experiment is presented in figure below.



Fig. 9. Block diagram of the experimental setup

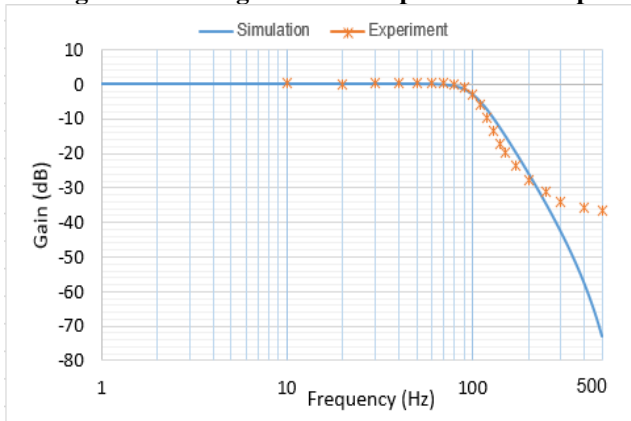


Fig. 10. Frequency response of bandpass filter

As the figures shown, the responses of the digital filters do not fit into the simulated curves. However, the attenuation of the digital bandpass filter response at 500 Hz reached to -40 dB instead of -10 dB in the analog bandpass filter.

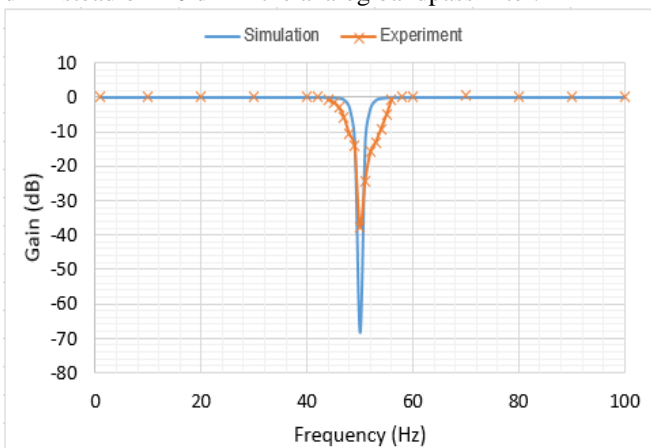


Fig. 11. Frequency response of bandstop filter

At the frequency of 50 Hz, the attenuation coefficient of the digital bandstop filter reached to -40 dB, the same coefficient as the analog bandstop filter, means the amplitude of the power line noise is reduce more than 100 times compared with the ECG signal from the electrodes. Because of the limitation of the ADC resolution and the step of the tuned frequencies from the generator, the minimum voltage can be read is 5 mV and the tuned frequency step is 1 Hz, the attenuation coefficient could not be measured much more precisely.

III. RESULTS & DISCUSSION

Figure 12 shows the signal measured by NI ELVIS II of lead I output from the differential amplifier. Because of the same gain coefficient of the 8 channels, the lead I represents the other channels as well. With the gain of 120, the amplitude of the signal reaches to 0.14Vp-p.

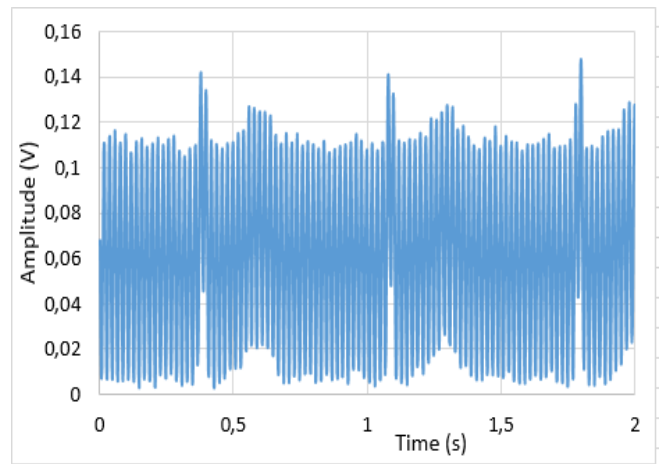


Fig. 12. The signal after differential amplifier

Although peak of the signal is indicated, the noise is still very strong. The ambient of the noise reaches to 110 mV approximately. The figure 13 shows the spectrum analysis that the noise frequency mainly come from 50 Hz, consistent with the power line noise. Another noise can be observed is the DC noise with the amplitude of -15 dB, much higher than power line noise.

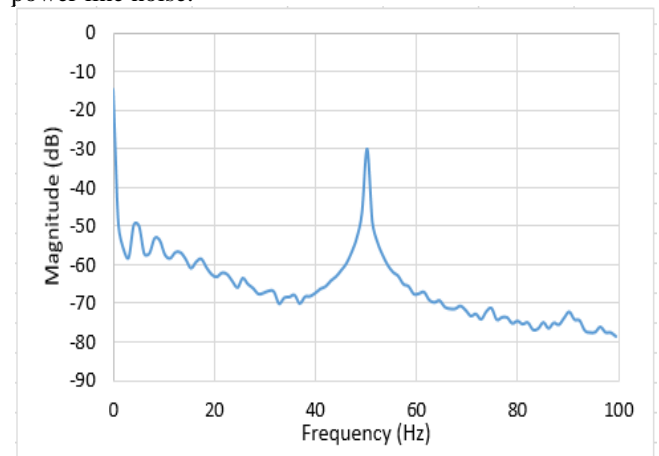


Fig. 13. The spectrum after differential amplifier

After go through the highpass filter, the DC component is eliminated as shown in figure 14. The baseline of the ECG signal, now, locates on the 0 in the graph. Since the highpass filter is the passive filter, the amplitude of the signal is reduced slightly as 0.1V. Nevertheless, the effects of the power line noise still presented.

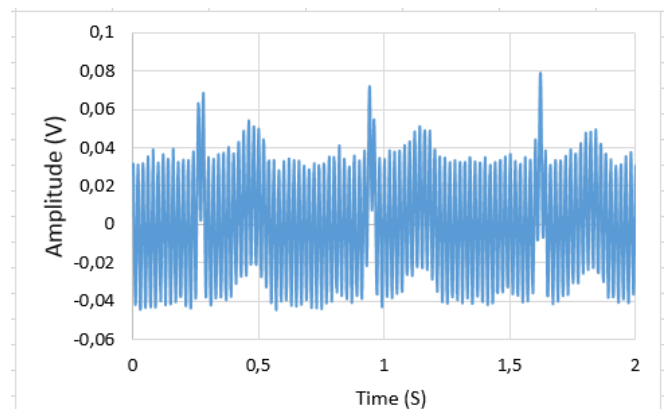


Fig. 14. The signal after highpass filter

Since the highpass filter cutoff at 0.16 Hz, the power line noise of 50 Hz could not be attenuated. The spectrum shown in figure 15 indicated that the DC noise was reduced while the power line noise still occurred at -40 dB level.

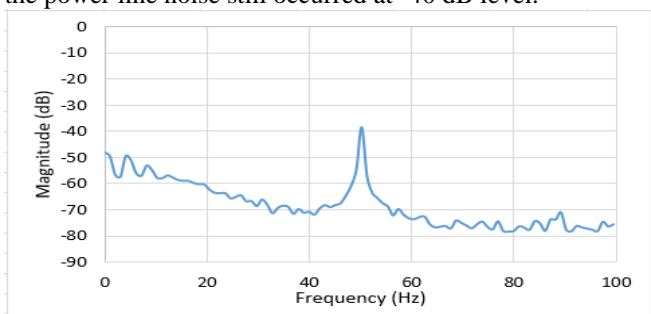


Fig. 15. The spectrum after highpass filter

The signal is amplified to 0.6Vp-p with the gain of 15 dB designed in active lowpass filter. Because of the noise level in high frequency range indicated in spectrum shown in the figure 15 and 13 is too low compared with the power line noise, the SNR of the signal seems does not improved.

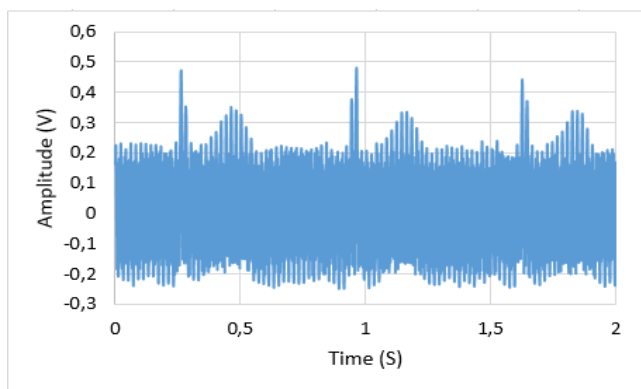


Fig. 16. The signal after lowpass filter

The high frequency noise level output from the active lowpass filter still presents at -60 to -70 dB, similarly to the noise level of the signal output from the highpass filter even the gain is increasing. This means, in the range of 1-100 Hz, the signal of the ECG is conserved.

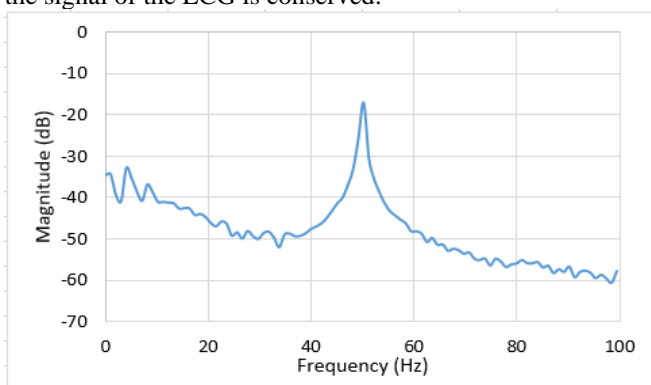


Fig. 17. The spectrum after lowpass filter

The power line noise is reduced greatly when the ECG signal passed through the active bandstop filter, and the improvement of the SNR is shown in figure 18. The noise ambient is shorten as 0.03Vp-p approximately.

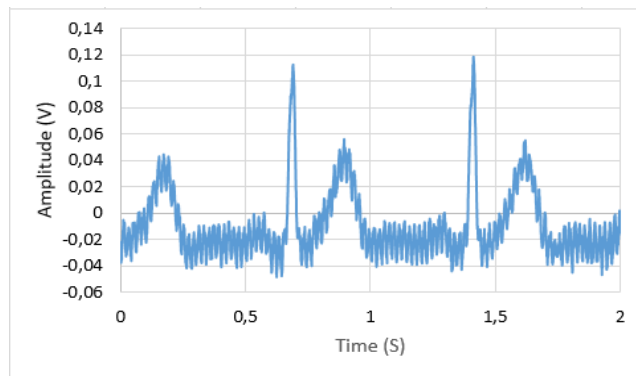


Fig. 18. The signal after bandstop filter

Compare to the spectrum of the signal output from the lowpass filter, the noise level of the power line is -38 dB while the signal level appeared as -40 dB, much better than the comparison of -15 dB with -35 dB, respectively. The amplitude of this signal in this stage obtained as 140 mV, much higher than the 30 mV amplitude of the power line noise.

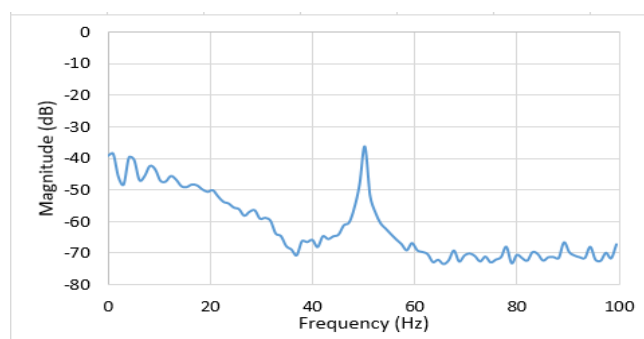


Fig. 19. The spectrum after bandstop filter

Since the signal's amplitude is still low, it is necessary to integrate an amplifier on the offset circuit to increase the signal how to adapt with the range of ADC input to enhance the measurement resolution. For this purpose, the ratio of R12/R11 is set as 10 with the value of R12 and R11 are 100 KΩ and 10 KΩ, respectively. The signal amplitude raised up to 1.2Vp-p approximately being shown in figure 20.

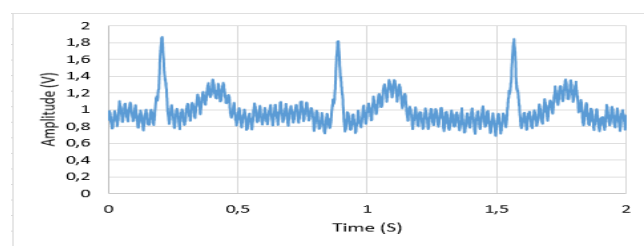


Fig. 20. The lead I analog signal

The spectrum of the signal is shown in figure 21. Because of the offset level, the spectrum of the signal appears the DC component. This DC component can be removed by the digital filter installed in software. The level of the power noise is the same as the noise contaminated in the signal output from the active bandstop filter.

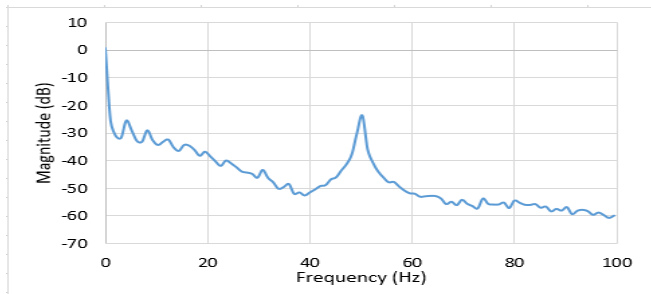


Fig. 21. The lead I spectrum

Figure 22 shows the user interface of the software displaying the graphs of the 12 leads measured from the volunteer person in which the detail of the lead I signal is extracted and shown in figure 23.



Fig. 22. The system software interface

As the figure 23 show, the noise level is reduced to 5 mV approximately compared with the amplitude signal of 1.2Vp-p. The noise mainly comes from the power line interference and the spectrum of the signal shown in figure 24 demonstrated that the 50 Hz noise presented in figure 15, 17, 19 and 21 is eliminated from the spectrum of the final signal.

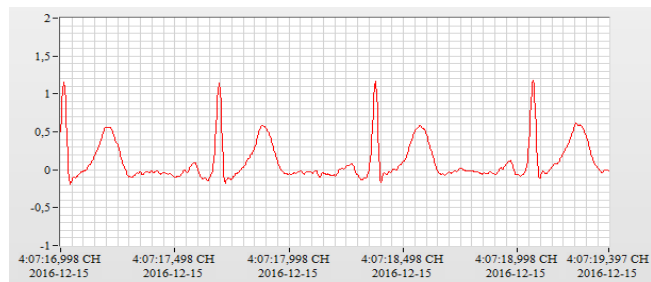


Fig. 23. The lead I signal after digital filters

The 50Hz noise level is deeply decreased because of the digital bandstop filter with the 6th order. Therefore, the performance of the system is improved with the SNR increased up to 26 dB approximately.

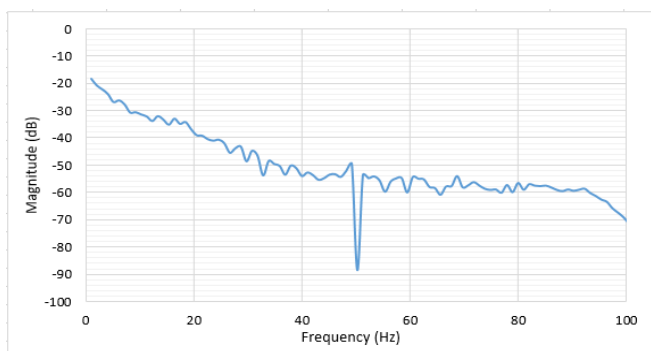


Fig. 24. The lead I spectrum after digital filters

The performance of system is evaluated by SNR value through a series of signal stages. The SNR value is determined from the formula [13]:

$$SNR = 20 \log_{10} \frac{V_{signal}}{V_{noise}} \quad (19)$$

The SNR has been improved from 1.4 dB to 27.6 dB at output signal as shown in table 3. As the measurement data, the SNR is really improve after attenuation of the power line noise.

Table- III: The SNR of signal through stages

Stages	Signal (V)	Noise(V)	SNRdB
Differential opamp	0.13	0.11	1.4
Highpass filter	0.11	0.07	3.9
Lowpass filter	0.65	0.4	4.2
Bandstop filter	0.14	0.025	14.9
Analog output	1.2	0.2	15.5
System output	1.2	0.05	27.6

To evaluate the delay of 8 signal channels, the R peak of lead I was chosen as the original for comparison with the remaining 7 channels. The delay time is shown in the following table:

Table- IV: The delay time among 8 channels

Lead	Delay time (s)
L1	0
L3	0,00571
V1	0,01143
V2	0,01429
V3	0,01143
V4	0,00286
V5	0,00286
V6	0,00286

Since one normal R-R cycle has duration of 0.6-1 seconds (heart rates range from 60-100 bpm) [15], the delay time is small enough to demonstrate that the ECG data is acquired in real time. Figure 25 shows the graphs of the three limb leads and the figure 26 presents the three augmented limb leads while the figure 27 plots the six precordial leads in detail. The graphs figures out the high SNR and low noise with the characteristic waves of the ECG is shown clearly. The graphs also indicated the synchronization of the signal in time scale.

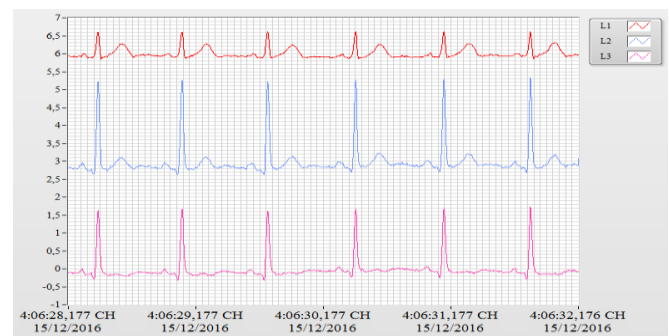


Fig. 25. The three limb leads

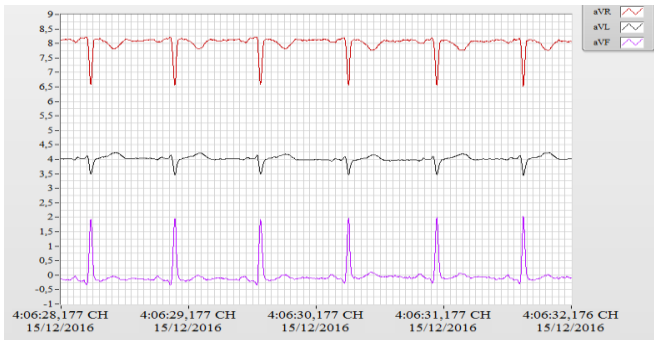


Fig. 26. The three augmented limb leads

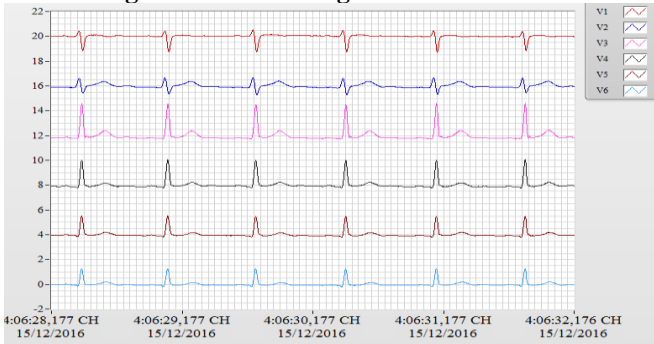


Fig. 27. The six precordial leads

IV. CONCLUSION

In this paper, a design of multichannel ECG acquisition system has been presented and demonstrated. The system measures signals from 12 ECG leads consequently in real time with sampling frequency of 350 Hz and displays them on the graphs with time delay of 5 milliseconds maximum. The original ECG signal is amplified and processed analogously with 14.6 dB then converted and digitalized processed through the digital filters. Through out the analog and digital processing, the ECG signal possibly observed in frequency range of 0.05 Hz to 100 Hz. The collected data is observed and possibly stored into file formatted as TDMS to reuse in other applications such as analysis or review software as well as telemedicine applications. The system is compact, portable and low-cost since the application based on commercial microcontroller module of Arduino. Practically, for evaluation, this system was used to measure the real ECG signals from a volunteer. The ECG wave is possibly reconstructed based on the raw data with adjustable parameters for signal processing such as frequency range, filter order as well as sampling frequency. The performance of system is evaluated by SNR value, which has increased from 1.4 dB to 27.6 dB at output signal. Based on this opened-system, various applications in biomedical diagnosis based on cardiovascular signal analysis are promised in the near future.

ACKNOWLEDGMENT

This work is financially supported by the program named as B2017-MHN.01 of Vietnam Ministry of Education and Training.

REFERENCES

1. Majd AlGhatrif, MD1 and Joseph Lindsay, MD2, "A brief review: history to understand fundamentals of electrocardiography", published online 2012 Apr 30.
2. Lieberman, Karen MS, CRNP, "Interpreting 12-Lead ECGs: A Piece by Piece Analysis", October 2008, Volume 33 Number 10 , p 28 - 35.

3. Dr Kofi Amu-Darko, "An Introduction to the 12 lead ECG & Acute MI changes", Charles Curtis Memorial Hospital, October 2008.
4. Bob Page, "12-Lead ECG for Acute and Critical Care Providers", Chapter 1 - Lead Placement and Acquisition (pages 1 -14), 2006 by Pearson Education, Inc. Upper Saddle River, NJ.
5. John E Madias, "On Recording the Unipolar ECG Limb Leads via the Wilson's vs the Goldberger's Terminals: aVR, aVL, and aVF", Published online 2008 Nov 1.
6. Gaetano D. Gargiulo, "True Unipolar ECG Machine for Wilson Central Terminal Measurements", Received 20 March 2015; Revised 13 May 2015; Accepted 13 May 2015.
7. L. A. Geddes and L. E. Baker, "Principles of Applied Biomedical Instrumentation", 3rd ed, New York, Wiley, 1989.
8. Ihor Gussak, Charles Antzelevitch, "Electrical Diseases of the Heart: Volume 2: Diagnosis and Treatment", Springer Science & Business Media, 23 May 2013 - 682 pages, chapter 14 - Surface Mapping and Magneto-Electrocardiography (pages 223 -238).
9. M.E Van Valkenburg, Analog Filter Design, published by Holt, Rinehart and Winston, 1982.
10. Doron Shmilovitz*, "Characteristics of modern nonlinear loads and their influence on systems with distributed generation", Int. J. Energy Technology and Policy, Vol. 5, No. 2, 2007.
11. Labview Makerhub, Retrieved from <https://www.labviewmakerhub.com/doku.php?id=libraries:linx:faq>, last accessed date 2/2/2017.
12. Sebastian Peryt, "Arduino and LabVIEW p.2 - Reading Analog Input", published in Arduino community, March 15, 2016.
13. Dr. Don H. Johnson, "Signal-to-noise ratio", Sponsored by: Eugene M. Izhikevich, Editor-in-Chief of Scholarpedia, accepted on: 12 February 2006.
14. Dobromir Dobrev, "Two-electrode low supply voltage electrocardiogram signal amplifier", March 2004, Volume 42, Issue 2, pp 272-276.
15. Nivedita Deshpande1, Dr. KavitaThakur2, Prof. A.S.Zadgaonkar3, "Assessment of systolic and diastolic cardiac cycle duration from speech analysis in the state of anger and fear", Conference: The First International Conference on Information Technology Convergence and Services, January 2012.
16. Elias Ebrahimzadeh, "ECG signals noise removal: selection and optimization of the best adaptive filtering algorithm based on various algorithms comparison", volume 27, issue 04, august 2015.
17. Yan Lina, Mana Sriyudthsak, "Design and Development of Standard 12-Lead ECG Data Acquisition and Monitoring System", 016 International Electrical Engineering Congress, iEECON2016, 2-4 March 2016, Chiang Mai, Thailand.

AUTHORS PROFILE



Son Nguyen Van is a lecturer of Faculty of Electronic Technology and Communication, Hanoi Open University. He received his B.E, M.S. degrees in Electronics and Telecommunications at Hanoi Open University, Vietnam



Duc Trinh Quang received his B.E, M.S. degrees in Control Engineering and Automation at HUST, Vietnam, and Ph.D. degrees (2012) in Tohoku Institute of Technolog, Sendai, Japan, he is lecturer of Electronics and Telecommunications at HUST, Vietnam



Giang Nguyen Hoai received his B.E, M.S. degrees in Information Technology at Budapest University of Technology and Economics, Hungary, and Ph.D. degrees (2009) in Electronics and Telecommunication from Hanoi University of Science and Technology (HUST). He is lecturer of Electronics and Telecommunications at Hanoi Open University, Vietnam

